

## X-ray production cross sections, intensity ratios, and centroid energy shifts of Ag $K$ and $L$ and Au $L$ x rays produced by $^{16}\text{O}$ beams of 12–50 MeV $^\dagger$

G. Bissinger

*East Carolina University, Greenville, North Carolina 27834*

P. H. Nettles\* and S. M. Shafroth

*University of North Carolina, Chapel Hill, North Carolina 27514  
and Triangle Universities Nuclear Laboratory, Durham, North Carolina 27706*

A. W. Waltner

*North Carolina State University, Raleigh, North Carolina 27607  
and Triangle Universities Nuclear Laboratory, Durham, North Carolina 27706  
(Received 21 August 1974)*

The 12–50-MeV  $^{16}\text{O}$  beam-induced  $K$  and  $L$  x rays of Ag and the  $L$  x rays of Au from thin targets were studied with a Si(Li) detector. Absolute  $K$  and  $L$  x-ray production cross sections were derived from measured x-ray yields and compared to available theoretical calculations for inner-shell Coulomb ionization cross sections. Inclusion of Coulomb repulsion, binding, and  $(Z_1/Z_2)^3$  effects in the plane-wave Born-approximation calculations gives good agreement with experimental values of  $\sigma_{KX}$  for Ag. The agreement between theory and experiment for  $L$ -shell ionization is not as good, possibly owing to the effects of multiple ionization on the fluorescence yield, although the energy dependence of  $\sigma_{LX}$  for Au is well reproduced. The energies of the Ag  $K\alpha$  and  $K\beta$  and Au  $L\alpha$ ,  $L\beta$ , and  $L\gamma$  lines were observed to change with beam energy as did the intensity ratios of these lines. HFS calculations for the Ag  $K\alpha$  and  $K\beta$  lines indicate that the observed shifts are probably associated with multiple  $M$ -, not  $L$ -, shell ionization.

### I. INTRODUCTION

Multiple ionization of the target atom by high-energy heavy ions ( $Z \geq 3$ ) and its effects on the energies of emitted characteristic x rays is now well established. Using Si(Li) detectors the effect appears as an upward shift in the energies of  $K$  (Refs. 1–4) and  $L$  (Ref. 5) x rays. With crystal spectrometers, it was possible to resolve structure in the heavy-ion-induced  $K$  x rays that could be attributed to simultaneous vacancies in the  $K$  and  $L$  shells<sup>6,7</sup> (plus  $M$ -shell vacancies). Recently, moreover, multiple ionization effects have also been observed for low-energy proton bombardment of N using Auger spectrometers.<sup>8</sup> Also observed are changes in the  $K\alpha/K\beta$ , etc., ratios.

The near-linear dependence of the energy shifts [observed with a Si(Li) detector] on the stopping power for the bombarding ion observed by Saltmarsh, Van der Woude, and Ludemann,<sup>9</sup> as well as the agreement obtained by Knudson, Burkhalter, and Nagel<sup>10</sup> with experimental Al  $K$  satellite/parent ratios using a direct Coulomb interaction in the impact-parameter formulation<sup>11,12</sup> for the production of simultaneous  $K$ - and  $L$ -shell vacancies, indicates that the observed multiple ionization is at least partly due to projectile-target Coulomb interactions. Recent calculations of multiple ionization probabilities for Cu by Hansteen and Mosebekk<sup>13</sup> give quantitative agreement with measured satel-

lite/parent ratios for Fe. However, the effects of multiple ionization on fluorescence yields, total  $K$  and  $L$  x-ray production cross sections, and intensity ratios of characteristic x rays, etc., are still not well investigated.

### II. EXPERIMENTAL PROCEDURES

The experimental arrangement and data-analysis procedures have been described in detail elsewhere.<sup>14–16</sup> The Ag and Au targets [(30.9  $\pm$  3.5)  $\times 10^{-6}$  cm and (1.50  $\pm$  0.05)  $\times 10^{-6}$  cm, respectively, the latter evaporated onto a 20- $\mu\text{g}/\text{cm}^2$  C foil] were bombarded with nanoamp  $^{16}\text{O}^{4+–6+}$  beams of 12–50 MeV from the TUNL tandem Van de Graaff. The x rays were detected with two Si(Li) detectors of 200- and 540-eV resolution for a 5.9-keV line. Sample spectra produced by a 36-MeV  $^{16}\text{O}$  bombardment of the Au and Ag are shown in Fig. 1 for the higher-resolution detector. Data points were normalized to the integrated charge, after correcting for the beam-energy-dependent variation of the average charge state of the  $^{16}\text{O}$  beam emerging from the target.<sup>17</sup>

### III. RESULTS AND DISCUSSION

The measured x-ray intensities were converted to x-ray yields  $Y$ , after correcting for absorption and detector efficiency. These yields are then

used to find the total x-ray production cross section  $\sigma_x$  or the total ionization cross section  $\sigma$ , where

$$\sigma = \sigma_x \omega^{-1} \quad (1)$$

and  $\omega$  is the fluorescence yield. Values of  $\omega$  have been chosen from the literature, although there is reason to believe that these are not necessarily accurate for the case of  $^{16}\text{O}$  beams,<sup>18</sup> where there is clear evidence in the data, as here, of multiple ionization of the target atoms.

#### A. K- and L-shell ionization cross sections for Ag

The values of  $\sigma_{KX}$  derived from the measured K x-ray yields, averaged for the two detectors, are given in Table I. These measurements are compared with the plane-wave Born-approximation<sup>19</sup> (PWBA), binary-encounter approximation<sup>20</sup> (BEA), and semiclassical approximation<sup>11,12</sup> (SCA) predictions [theoretical values corrected for fluorescence yield,  $\omega_K = 0.830 \pm 0.025$  (Ref. 21)] in Fig. 2. There are three PWBA curves shown in Fig. 2: (i) from a presently available tabulation<sup>22</sup> of K-shell ionization cross sections with a screening constant  $\theta_K = 0.86$ , (ii) the same as (i) but corrected for Coulomb-repulsion and binding-energy effects,<sup>23</sup> and (iii) as in (ii) but with terms in the plane-wave expansion to  $(Z_1/Z_2)^3$ ,<sup>24</sup> where  $Z_1$  and  $Z_2$  are the projectile and target atomic numbers, respectively. The added corrections in (iii) give improved agreement with the experimental values of  $\sigma_{KX}$ , although there appears to be systematic deviations between theory and experiment at the lowest and highest projectile energies.

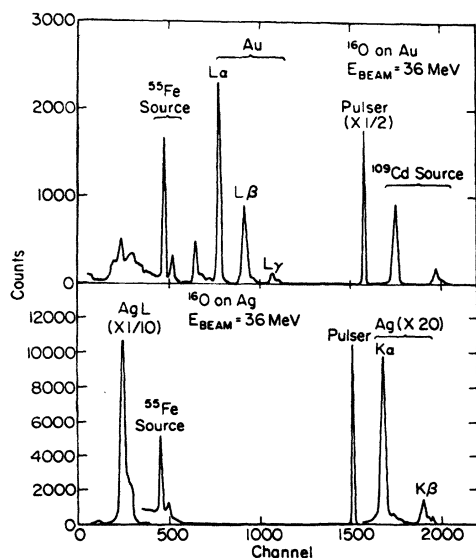


FIG. 1. Pulse-height spectra for 36-MeV  $^{16}\text{O}$  bombardment of Ag and Au.

TABLE I. Ag K and L x-ray production cross sections for  $^{16}\text{O}$  bombardment.

Incident energy (MeV)	$\bar{E}^a$ (MeV)	Average <sup>b</sup> charge state	$\sigma_{KX}$ (b)	$\sigma_{LX}$ (kb)
12.0	11.4	5.99	$0.27 \pm 0.04$	$5.3 \pm 1.1$
18.0	17.4	6.53	$1.89 \pm 0.20$	$19 \pm 4$
24.0	23.4	6.86	$4.90 \pm 0.53$	$41 \pm 8$
30.0	29.4	7.08	$11.1 \pm 1.6$	$75 \pm 15$
36.0	35.5	7.24	$19.8 \pm 2.2$	$102 \pm 20$
42.0	41.5	7.39	$33.2 \pm 3.6$	$125 \pm 25$
50.0	49.5	7.50	$52.1 \pm 7.9$	

<sup>a</sup> Corrected for energy loss in target using tables in L. C. Northcliffe and R. F. Schilling, Nucl. Data A 7, 233 (1970).

<sup>b</sup> Reference 17.

Since the Ag L lines could not be resolved, a mean fluorescence yield  $\bar{\omega}_L$  was used to calculate theoretical values of  $\sigma_{LX}$  for Ag. The value used here was  $\bar{\omega}_L = 0.0659 \pm 0.0037$ .<sup>25</sup> Although it is expected that the various subshell contributions to the observed Ag L line will vary with beam energy, and the value of  $\bar{\omega}_L$  used here was measured for only one subshell vacancy distribution, Bambynek *et al.*<sup>21</sup> note that even drastic variations in these distributions do not strongly affect the values of  $\bar{\omega}_L$ . The experimental values for  $\sigma_{LX}$  are listed in Table I. The cross-section data are compared with PWBA theoretical predictions<sup>22</sup> in Fig. 3. Clearly, there are large discrepancies between experimental results and theory, with experimental values of  $\sigma_{LX}$

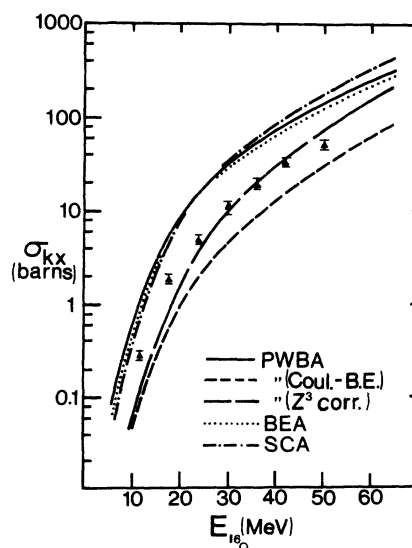


FIG. 2. Comparison of theoretical predictions of  $\sigma_{KX}$  ( $\omega_K = 0.830$ ) with experimental results obtained for  $^{16}\text{O}$  bombardment of Ag.

falling below theoretical predictions at 12 MeV and rising above predictions for higher beam energies. The latter behavior is probably due to increases in the fluorescence yield associated with multiple ionization.

#### B. Au $L$ x-ray production cross section

With relatively low-resolution spectra, as here, it is very difficult to extract reliable subshell ionization cross sections; hence, theoretical values<sup>22</sup> for  $\sigma_{L1}$ ,  $\sigma_{L2}$ , and  $\sigma_{L3}$  were used to calculate  $\sigma_{LX}$  for comparison with experiment. In Fig. 4 the experimental values of  $\sigma_{LX}$  (also listed in Table II) are compared with those calculated from PWBA. The subshell fluorescence yields and Coster-Krönig fractions employed in the calculations are from Ref. 26. The measured energy dependence of  $\sigma_{LX}$  is well reproduced by the PWBA values for  $\sigma_{LX}$  but the agreement in magnitude is not quite as good, possibly owing to inaccurate fluorescence-yield values.<sup>19</sup> However, these same values were used in an earlier study<sup>28</sup> of proton-induced Au  $L$  x rays and gave quite good agreement with experiment there, implying possible fluorescence-yield variations associated with the projectile.

#### C. Ag $K\alpha/K\beta$ and $K\beta_{1,3}/K\beta_2$ intensity ratios

In 2–30-MeV proton bombardment of Ag, the  $K\alpha/K\beta$  ratio did not vary with beam energy.<sup>15</sup> This is not the case for  $^{16}\text{O}$  beams, where variations over 50% are seen in the energy range of 12–50 MeV. The values observed in this work at low  $^{16}\text{O}$

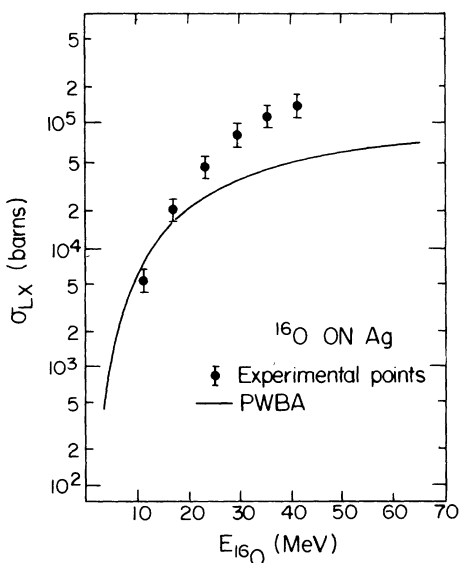


FIG. 3. Comparison of theoretical predictions of  $\sigma_{LX}$  ( $\bar{\omega}_L = 0.0659$ ) with experimental results obtained for  $^{16}\text{O}$  bombardment of Ag.

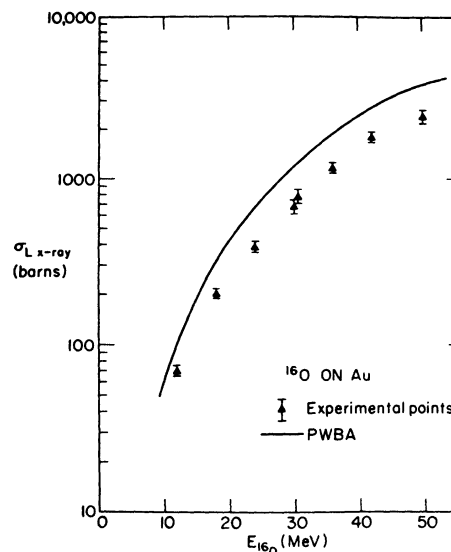


FIG. 4. Comparison of theoretical predictions of  $\sigma_{LX}$  (fluorescence yields and Coster-Krönig fractions from Ref. 26) with experimental results obtained for  $^{16}\text{O}$  bombardment of Au.

energies are higher than those observed in proton bombardment, while at the highest  $^{16}\text{O}$  energies they are lower. This is shown in Fig. 5(a). No significant variation with beam energy is seen in the  $K\beta_{1,3}/K\beta_2$  ratio [Fig. 5(b)], which lies below the theoretical value<sup>27</sup> of 6.01. The  $K\beta_{1,3}$  and  $K\beta_2$  components are expected to comprise 99% of the  $K\beta$  intensity.<sup>27</sup>

The energy dependence of the Ag  $K\alpha/K\beta$  ratio is not fully understood. It is *not* due to differential absorption in the target as the  $K\beta$  line(s) is shifted at increased stages of ionization above the  $K$  edge in Ag. Self-absorption in the target is so small that this effect is not a significant contribution. In any case, the effect observed is opposite to that expected from self-absorption. Multiple ionization of the  $M$  shell is a possible explanation since the

TABLE II. Au  $L$  x-ray production cross sections for  $^{16}\text{O}$  bombardment.

Incident <sup>a</sup> energy (MeV)	$\sigma_{LX}$ (b)
12	71 ± 5
18	203 ± 14
24	390 ± 28
30	680 ± 70
36	1190 ± 85
42	1810 ± 130
50	2420 ± 240

<sup>a</sup> Total projectile energy loss in target ranged from 59 to 73 keV and has been disregarded.

peak in  $\sigma_M$  lies below the projectile energy range covered here. Also to be considered are possible relative variations of  $\omega_K$  for various members of the  $K$  series.

#### D. Au $L\alpha/L\beta$ and $L\alpha/L\gamma$ intensity ratios

The 0.5–30-MeV proton-induced Au  $L$  x-ray intensity ratios<sup>28</sup> showed noticeable variations, particularly from 0.5–5-MeV, which is the approximate  $^{16}\text{O}$  beam velocity region covered here. In Figs. 6(a) and 6(b) the energy dependences of  $L\alpha/L\beta$  and  $L\alpha/L\gamma$  are displayed for 12–50-MeV  $^{16}\text{O}$  beams, along with the 0.5–3.0-MeV proton-beam (8–48-MeV  $^{16}\text{O}$  velocity equivalent) results for comparison. At  $E(^{16}\text{O}) \geq 24$  MeV, the results for the two projectiles agree within error, while below this energy the proton ratios lie above the  $^{16}\text{O}$  ratios. This discrepancy increases with decreasing projectile velocity.

#### E. Energy shifts in Ag $K\alpha$ and $K\beta$ lines

Although the resolution of the Si(Li) detector is not sufficient to resolve the  $K\alpha_1$ - $K\alpha_2$  and  $K\beta_1$ - $K\beta_3$  doublets, still there is useful information in even relatively low-resolution data since the observed centroid shifts can be partially interpreted with the aid of Hartree-Fock-Slater (HFS) calculations.<sup>29</sup> These have been performed for the case of Ag  $K\alpha$  and  $K\beta$  for many ionization configurations. To reduce relativistic effects in the HFS calculated

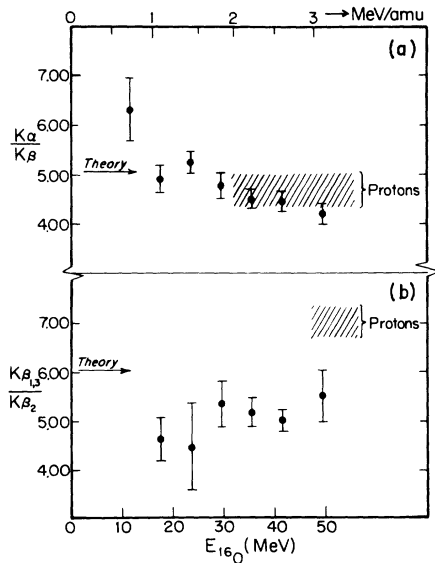


FIG. 5. (a) Ag  $K\alpha/K\beta$  ratio vs  $E(^{16}\text{O})$ . (b) Ag  $K\beta_{1,3}/K\beta_2$  ratio vs  $E(^{16}\text{O})$ . The shaded regions indicate the results of Bissinger *et al.* (Ref. 15) for 2–30-MeV proton bombardment of Ag. The arrows labeled theory are taken from Scofield (Ref. 27) and are ratios of radiative widths.

binding energies, only the differences  $\delta K\alpha \equiv K\alpha$  (multiply ionized configuration) –  $K\alpha$  (single  $K$  vacancy) and  $\delta K\beta$  (similar definition) are shown in Figs. 7(a) and 7(b). The calculated values of  $\delta K\alpha, \beta$  are to be compared to the equivalent experimental quantities in Fig. 8, i.e.,  $\delta K\alpha = K\alpha(^{16}\text{O}) - K\alpha(^{109}\text{Cd})$ . The experimental values of  $\delta K\alpha$  hover around 20–30 eV, while  $\delta K\beta$  increases from ~50 eV at 12 MeV to ~140 eV at 50 MeV. This result, which was somewhat surprising initially, can be explained by observing that multiple ionization of the  $M$  shell could easily cause the observed  $\delta K\alpha, \delta K\beta$  values, without requiring any additional  $L$  vacancies. It is also worth noting that the HFS calculations of  $\delta K\alpha$  show no significant variation (<3 eV) in the  $K\alpha$  energy for up to at least six  $3d$  vacancies.

The experimental values for  $\delta K\alpha$  and  $\delta K\beta$  imply that even at the highest projectile energies no major portion of  $K$ -shell ionization events are accompanied by simultaneous  $L$ -shell ionization, i.e.,  $K^{-1}, M^{-n}$  configurations dominate. At low projectile energies, the large variation in the  $K\alpha/K\beta$  ratio and the small values of  $\delta K\alpha, \beta$  both are strong evidence for multiple ionization of the  $M$  shell. It is possible to estimate the probability of simultaneous  $K$ - and  $L$ -shell ionization from recent work of Hansteen and Mosebekk<sup>13</sup> and McGuire

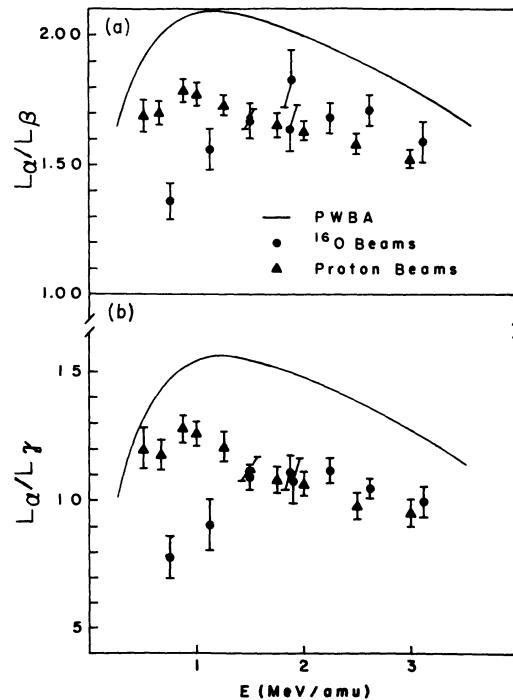


FIG. 6. (a) Au  $L\alpha/L\beta$  ratio vs  $E(^{16}\text{O})$ . (b) Au  $L\alpha/L\gamma$  ratio vs  $E(^{16}\text{O})$  [equivalent-velocity proton-beam results from previous work are shown in both (a) and (b)].

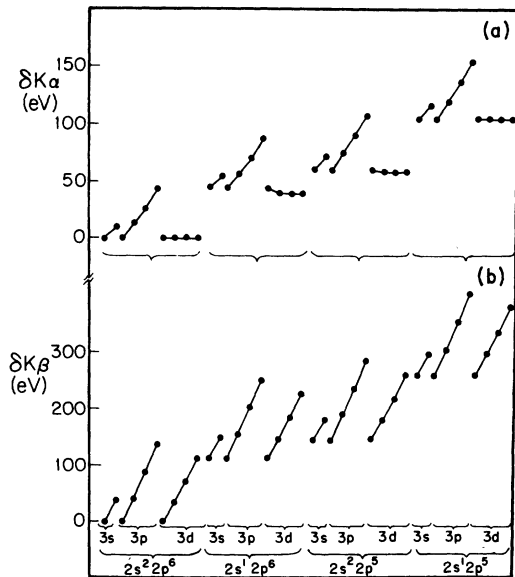


FIG. 7. (a) HFS calculations of  $\delta K\alpha \equiv K\alpha$  (multiply ionized configuration)  $-K\alpha$  (single  $K$  vacancy) for successive removal of two electrons (maximum of six removed). (b) HFS calculations of  $\delta K\beta$ .

and Richard.<sup>30</sup> Using an impact-parameter representation for inner-shell ionization, but with different approaches, both predict simultaneous  $K$ - and  $L$ -shell ionization less than 1% of the time in the projectile energy range of this experiment.

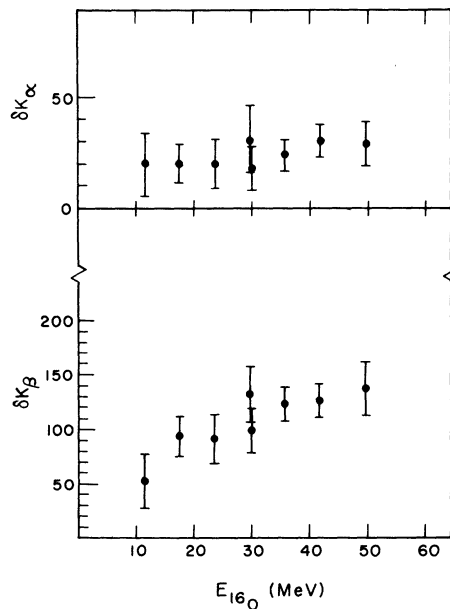


FIG. 8. Experimental energy shifts of  $\text{Ag}K\alpha$  and  $K\beta$  for  $^{16}\text{O}$  bombardment of Ag (in eV).

#### F. Energy shifts in Au $L\alpha$ , $L\beta$ , and $L\gamma$ lines

A facile interpretation of observed centroid shifts in the Au  $L\beta$  and  $L\gamma$  lines (shown in Fig. 9, along with  $L\alpha$ ) is not possible owing to independent and simultaneous centroid shifts associated with (a) multiple ionization, (b) relative variations in the various  $L$ -subshell ionization cross sections, and (c) possible relative variations in fluorescence yields and Coster-Krönig fractions implied by (a). Even  $L\alpha$  can be affected by (c). It is still informative to compare the observed centroid shifts with those obtained for incident protons<sup>28</sup> with the same velocities, however. In all cases the  $L\alpha$  and  $L\beta$  centroid energies are higher for  $^{16}\text{O}$  bombardment, and in the case of  $L\beta$  and  $L\gamma$  there are definite upward shifts as the  $^{16}\text{O}$  energy is increased. The latter shifts are almost certainly due to multiple ionization. Also included in Fig. 9 are centroid energies for  $L\beta$  and  $L\gamma$  calculated from PWBA  $L$ -subshell cross sections.<sup>28</sup>

Calculations by Mokler<sup>5</sup> have shown that simultaneous  $L$ - and  $M$ -shell ionization in the case of Au will lead to upward shifts in the  $L\alpha$  line of  $\sim 20$  eV for each  $M$  vacancy. This is approximately the shift observed in  $L\alpha$  going from 12- to 50-MeV oxygen beams.

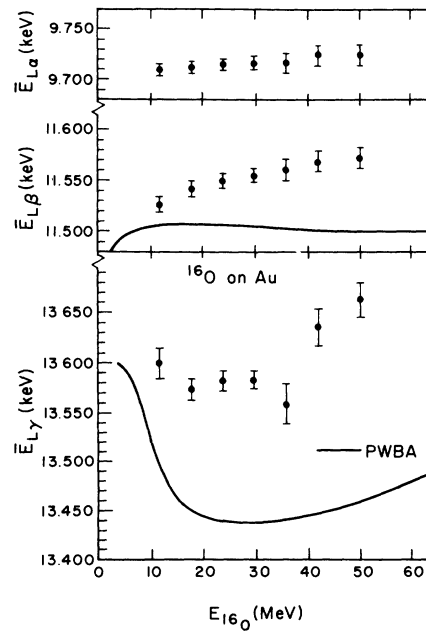


FIG. 9. Experimental centroid energies for the Au  $L\alpha$ ,  $L\beta$ , and  $L\gamma$  lines for  $^{16}\text{O}$  bombardment of Au. Also shown are the PWBA prediction for the  $L\beta$  and  $L\gamma$  centroid energies.

## IV. SUMMARY

The Ag  $K$  and Au  $L$  x-ray production cross-section measurements are observed to be in reasonably good agreement with theoretical PWBA predictions, particularly in the case of Ag, where corrections for binding, Coulomb deflection, and inclusion of  $(Z_1/Z_2)^3$  in the plane-wave expansion have been applied. This is somewhat surprising in view of the fact that multiple ionization can strongly affect<sup>18</sup> the value of  $\omega_K$ . If it is presumed that the principal effect of multiple ionization is to increase  $\omega_K$ , as observed in the case of <sup>16</sup>O on Ne,<sup>18</sup> then for Ag  $\omega_K$  can only increase by ~20% and the agreement between experiment and theory is understandable. Correction for recoil contributions<sup>31</sup> to the measured x-ray yields is not expected to be of any importance for these measurements. Considerably poorer agreement between measured Ag  $L$  x-ray yields and PWBA predictions is observed, particularly at higher projectile energies. Possibly this is due to multiple ionization and its concomitant effects on fluorescence yields.

The observed Ag  $K\alpha/K\beta$  ratios varied quite markedly with energy, the highest values occurring

at the lowest beam energies. Similar behavior<sup>32</sup> has been observed on <sup>16</sup>O beam bombardment of lower- $Z$  targets. This behavior, combined with observed energy shifts in the Ag  $K\alpha$  and  $K\beta$  lines at low projectile energies, would seem to imply that multiple ionization of the  $M$  shell is occurring. Observed energy shifts in the Au  $L\alpha$  line indicate multiple  $M$ -shell ionization is the dominant factor in 12–50-MeV <sup>16</sup>O bombardment of Au also. Surprisingly, the Au  $L\alpha/L\beta$  and  $L\alpha/L\gamma$  ratios converge to proton-induced results at projectile velocities corresponding to 1.5 MeV/amu or greater, even though the  $L$  x rays of Au still indicate considerable multiple ionization is occurring in this energy region.

## ACKNOWLEDGMENTS

We are grateful to Dr. Eugen Merzbacher for encouragement and helpful discussion, to Dr. B. H. Choi for providing the PWBA calculations of intensity ratios and energy shifts for the Au  $L$  x rays, and to Dr. George Basbas for providing the  $(Z_1/Z_2)^3$ -corrected PWBA calculations.

†Work performed under the auspices of the U. S. Atomic Energy Commission.

\*Present address: Scientific Atlanta, Box 13654, Atlanta, Ga.

<sup>1</sup>P. Richard, I. L. Morgan, T. Furuta, and D. Burch, Phys. Rev. Lett. **23**, 1009 (1969).

<sup>2</sup>P. Richard, T. I. Bonner, T. Furuta, I. L. Morgan, and J. R. Rhodes, Phys. Rev. A **1**, 1044 (1970).

<sup>3</sup>D. Burch and P. Richard, Phys. Rev. Lett. **25**, 983 (1970).

<sup>4</sup>G. A. Bissinger, P. H. Nettles, S. M. Shafroth, and A. W. Waltner, Bull. Am. Phys. Soc. **16**, 545 (1971).

<sup>5</sup>P. H. Mokler, Phys. Rev. Lett. **26**, 811 (1971).

<sup>6</sup>A. R. Knudson, D. J. Nagel, P. G. Burkhalter, and K. L. Dunning, Phys. Rev. Lett. **26**, 1149 (1971).

<sup>7</sup>D. Burch, P. Richard, and R. L. Blake, Phys. Rev. Lett. **26**, 1355 (1971).

<sup>8</sup>N. Stolterfoht, Phys. Lett. **41A**, 400 (1972).

<sup>9</sup>M. J. Saltmarsh, A. Van der Woude, and C. A. Ludemann, Phys. Rev. Lett. **29**, 329 (1972).

<sup>10</sup>A. R. Knudson, D. J. Nagel, and P. G. Burkhalter, *Proceedings of the International Conference on Inner-Shell Ionization Phenomena, Atlanta, Georgia, 1972*, Conf.-720404 (U. S. Atomic Energy Commission, Oak Ridge, Tenn., 1973).

<sup>11</sup>J. Bang and J. M. Hansteen, K. Dan. Vidensk. Selsk. Mat.-Fys. Medd. **31**, No. 13 (1959).

<sup>12</sup>J. M. Hansteen and O. P. Mosebekk, Z. Phys. **234**, 281 (1970); Nucl. Phys. A **201**, 541 (1973).

<sup>13</sup>J. M. Hansteen and O. P. Mosebekk, Phys. Rev. Lett. **29**, 1361 (1972).

<sup>14</sup>G. A. Bissinger, J. M. Joyce, E. J. Ludwig, W. S. McEver, and S. M. Shafroth, Phys. Rev. A **1**, 841 (1970).

<sup>15</sup>G. Bissinger, S. M. Shafroth, and A. W. Waltner, Phys. Rev. A **5**, 2046 (1972).

<sup>16</sup>G. A. Bissinger, A. B. Baskin, B. H. Choi, S. M. Shafroth, J. M. Howard, and A. W. Waltner, Phys. Rev. A **6**, 545 (1972).

<sup>17</sup>J. B. Marion and F. C. Young, *Nuclear Reaction Analysis* (North-Holland, Amsterdam, 1968), p. 43.

<sup>18</sup>D. Burch, W. B. Ingalls, J. S. Risley, and R. Heffner, Phys. Rev. Lett. **29**, 1719 (1972).

<sup>19</sup>E. Merzbacher and H. W. Lewis, in *Handbuch der Physik*, edited by S. Flügge (Springer, Berlin, 1958), Vol. 34, p. 166.

<sup>20</sup>J. D. Garcia, Phys. Rev. A **1**, 280 (1970); **1**, 1402 (1970).

<sup>21</sup>W. Bambynek *et al.*, Rev. Mod. Phys. **44**, 716 (1972).

<sup>22</sup>G. S. Khandelwal, B. H. Choi, and E. Merzbacher, At. Data **1**, 103 (1969); **5**, 291 (1973).

<sup>23</sup>W. Brandt, R. Laubert, and I. Sellin, Phys. Rev. **151**, 56 (1966).

<sup>24</sup>G. Basbas, W. Brandt, and R. Laubert (unpublished).

<sup>25</sup>L. E. Bailey and J. B. Swedlund, Phys. Rev. **158**, 6 (1967).

<sup>26</sup>R. W. Fink, R. C. Jopson, H. Mark, and C. D. Swift, Rev. Mod. Phys. **38**, 513 (1966).

<sup>27</sup>J. H. Scofield, Phys. Rev. **179**, 9 (1969).

<sup>28</sup>S. M. Shafroth, G. Bissinger, and A. W. Waltner, Phys. Rev. A **7**, 566 (1973).

<sup>29</sup>F. Herman and S. Skillman, *Atomic Structure Calculations* (Prentice-Hall, Englewood Cliffs, N. J., 1963).

<sup>30</sup>J. H. McGuire and P. Richard, Phys. Rev. A **8**, 1374 (1973).

<sup>31</sup>K. Taulbjerg, B. Fastrup, and E. Laegsgaard, Phys. Rev. A **8**, 1814 (1973).

<sup>32</sup>D. Burch (private communication).